Available online at www.sciencedirect.com
SCIENCE DIRECT®
Journal of Power Sources 124 (2003) 330–337
JOURNAL OF POWER SOURCES
www.elsevier.com/locate/jpowsour

Sol–gel MnO_2 as an electrode material for electrochemical capacitors

Ravinder N. Reddy, Ramana G. Reddy*

Department of Metallurgical and Materials Engineering, The University of Alabama, Box 870202, Tuscaloosa, AL 35487, USA

Abstract

MnO_2 was synthesized by the sol–gel method. Two forms of MnO_2, namely xerogel and ambigel, were prepared by reduction of $NaMnO_4$ and $KMnO_4$ with sodium fumarate. The synthesized products were characterized using X-ray diffraction (XRD), Brunauer–Emmet–Teller (BET), scanning electron microscopy (SEM), thermogravimetric analysis (TGA) and chemical analysis. Electrochemical characterization was carried out using cyclic voltammetry by a three electrode system consisting of saturated calomel electrode as reference electrode, platinum mesh as a counter electrode, and sol–gel prepared MnO_2 mounted on Ti mesh used as working electrode. Aqueous NaCl, KCl, Na_2SO_4 and LiCl solutions were used as electrolytes. The ambigel form of MnO_2 showed high capacitance compared to that of the xerogel form of MnO_2. Maximum capacitance of 130 F/g was obtained at a scan rate of 5 mV/s for the ambigel form of MnO_2 in a 2 M NaCl solution. Effect of NaCl concentration on the capacitance of MnO_2 was studied. Stability of MnO_2 was studied up to 800 cycles.

Keywords: MnO_2; Xerogel; Ambigel; Pseudocapacitors

1. Introduction

Electrochemical capacitors are charge storage devices which have higher energy density than conventional dielectric capacitors and have higher power density than batteries [1–9]. Electrochemical capacitors fill the gap between batteries and conventional capacitors. Electrochemical capacitors are also known as supercapacitors, ultracapacitors, gold capacitors or power capacitors. Electrochemical capacitors are used as back-up memory for electronic devices such as VCR circuits, CD players, cameras, computers, clocks, clock radios, telephones, electronic toys, fire/smoke alarms and office equipment. Electrochemical capacitors are also used in hybrid electric vehicles in combination with batteries as they have higher power density than batteries for load leveling. Electrochemical capacitors in combination with batteries occupy less space and are light, have excellent cold weather starting and increased battery life. Other uses of electrochemical capacitors include regenerative breaking, unmanned monitoring units, uninterruptible power supplies (UPS), and high power lasers.

Electrochemical capacitors are classified into two types, electrochemical double layer capacitors (EDLC's) and capacitors based on pseudocapacitance. In electrochemical double layer capacitors, the charge is separated across the interface between the electrode and the electrolyte. Carbon having high surface area of the order of 2500 m^2/g is used as the electrode. Both aqueous and non-aqueous based solutions are used as electrolytes. The energy storage mechanism is the formation of double layer at the electrode and electrolyte interface. Specific capacitance of 280 and 120 F/g, respectively, can be achieved in aqueous and non-aqueous electrolytes with maximum voltages of 1 and 3 V, respectively [10]. In psuedocapacitors, transition metal oxides are used as electrode material. Transition metal oxides can be prepared in high surface area form, exist in several oxidation states, and some transition metal oxides are conductors. Aqueous based solutions are used as electrolytes in pseudocapacitors. In pseudocapacitors, Faradiac charge transfer occurs between electrolyte and electrode in contrast to electrostatic nature of opposite charges in double layer capacitors. Capacitance in pseudocapcitors arises due to the progressive redox reactions between several oxidation states. These redox transitions occur at the surface and bulk of transition metal oxides with the application of voltage.

Specific capacitance value of 720 F/g was obtained using amorphous ruthenium oxide as electrode in pseudocapacitors at 2 mV/s scan rate in H_2SO_4 electrolyte [11,12]. $RuO_2{\cdot}xH_2O$ is an ideal material suitable as an electrode for pseudocapacitor. However, hydrous ruthenium oxide is very expensive. Hence, efforts are made to replace ruthenium oxide by other transition metal oxides as electrodes in electrochemical capacitors. MnO_2 appears to be a promising

* Corresponding author. Tel.: +1-205-348-1740; fax: +1-205-348-2164.
E-mail address: rreddy@coe.eng.ua.edu (R.G. Reddy).

0378-7753/$ – see front matter © 2003 Elsevier B.V. All rights reserved.
doi:10.1016/S0378-7753(03)00600-1

material for electrochemical capacitors. The advantages of MnO_2 are its low cost and environmental friendly nature. Several researchers prepared MnO_2 from different starting materials for its use as electrode material in electrochemical capacitors. Lee et al. [13] prepared MnO_2 by thermal decomposition of $KMnO_4$ at different temperatures and proposed non-corrosive KCl as electrolyte. Lee et al. [14] prepared MnO_2 by co-precipitation method involving $KMnO_4$ and manganese acetate. Jeong and Manthiram [15] prepared MnO_2 by reduction of $KMnO_4$ by aqueous solution of potassium borohydride (KBH_4), sodium dithionide ($Na_2S_2O_4$) and sodium hypophosphite ($NaH_2PO_2{\cdot}H_2O$). In this study, MnO_2 was prepared from sol–gel method in two forms as: xerogel and ambigel. Sol–gel method has several advantages. Metal oxide powders can be prepared in homogenous, highly porous form and with particle size in submicron range. The application of both forms of synthesized MnO_2 as potential electrode material for electrochemical capacitors is investigated in this study.

2. Experimental

2.1. Preparation of xerogel MnO_2

MnO_2 was prepared from reduction of sodium permanganate ($NaMnO_4$) with sodium fumarate ($Na_2C_4H_2O_4$) mixed in the mole ratio of 3:1 [16,17]. An aqueous solution of sodium fumarate was added drop wise to the aqueous solution of $NaMnO_4$ while stirring the solution. Stirring was continued for 1 h and the mixture was vacuum degassed later for 60 min to remove CO_2. Vacuum degassing helped in homogenizing the solution. The solution was stirred for 24 h and 2.5 M H_2SO_4 was added drop wise with stirring. The solution is further stirred for 24 h and washed several times with distilled water to remove any soluble products. The product was filtered and dried at room temperature. The product $Na_xMnO_{2+y}{\cdot}nH_2O$ prepared by this method is termed as xerogel.

2.2. Preparation of ambigel MnO_2

The ambigel form of MnO_2 was prepared by removing the water present in the gel by exchanging the water with organic solvents. Initially, water present in the gel was stirred in acetone for 1 week. Acetone was replaced by cyclohexane and, finally, by hexane. The gel present in hexane was dried using vacuum for 12 h. The criteria for solvents exchange is solubility and surface tension. The solvent should be soluble in the previous solvent, and the surface tension should be lower than the previous one. The dried product is called ambigel. Fig. 1 shows the preparation flow chart of xerogel and ambigel forms of MnO_2. The ambigel form of potassium containing manganese oxide was prepared starting from $KMnO_4$ and sodium fumarate in the same way as described earlier.

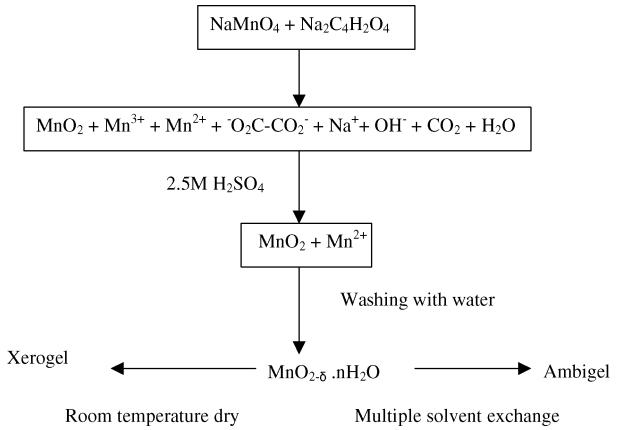

Fig. 1. Flow chart of preparation of xerogel and ambigel forms of MnO_2.

2.3. Characterization

The products were characterized using X-ray diffractometry (XRD), scanning electron microscopy (SEM), BET, ICP–ES and thermogravimetric analysis (TGA). XRD was performed using a Regaku D/MAX-2BX model. Particle size and morphology were analyzed using a Philip XL30 scanning electron microscope. TGA was performed using a Perkin–Elmer Pyris Diamond machine with a temperature increment of 10 °C/min under ambient conditions. TGA was used to find the amount of water present and also study the structural transformations of MnO_2. Surface area was determined by Brunauer–Emmet–Teller (BET) method using a Quanta Chrome, Chembet-3000 model. Initially, the sample was degassed for several hours at 300 °C under a flow of nitrogen. A mixture of nitrogen and helium were used as adsorbate gas. Alkali ions present were determined by inductively-coupled plasma emission spectroscopy. The solvent used for dissolution of MnO_2 was mixture of HNO_3 and H_2O_2. The mean oxidation state of Mn was obtained by chemical titration using ferrous ammonium sulfate [18]. As prepared powder was dissolved in a solution of H_2SO_4 and excess ferrous ammonium sulfate, so that all the Mn present would convert to Mn^{2+}. Excess Fe^{2+} ions were titrated against $KMnO_4$, which was previously standardized.

2.4. Electrode preparation and electrochemical characterization

Prepared powders were mixed with 23 wt.% of carbon black and 9 wt.% of PTFE binder. The mixture was pressed to make thin sheets using mortar and pestle. The sheets were rolled to get an approximate thickness of 100 μm. The electrode material was pressed on to Titanium mesh by means of a roller. The weight of electrode material was approximately 10 mg. Cyclic voltammetry was conducted using a EG&G potentiostat and galvanostat 273A employing a three electrode experimental setup. Platinum mesh and saturated calomel electrode were used as the counter and reference

electrodes, respectively. The electrolytes used in this study were NaCl, KCl, LiCl and Na_2SO_4 with varying concentration. The scan rate of 5 mV/s in the range of 0.0–1.0 V was used in every measurement unless otherwise mentioned. Specific capacitance (F/g) is calculated as the current divided by the scan rate and is normalized to 1 g of active material.

3. Results and discussion

Generally, sol–gel preparation involves the hydrolysis and condensation of metal ions. The problem in preparing MnO_2 using sol–gel method is lack of a stable Mn(IV) precursor. This can be circumvented by in-situ formation of Mn(IV) via reduction of $NaMnO_4$ with sodium fumarate [16]. When $NaMnO_4$ is reduced with sodium fumarate, Mn^{3+} and Mn^{2+} ions are formed. Sulfuric acid disproportionate Mn^{3+} into Mn^{4+} and soluble Mn^{2+} ions. Soluble Mn^{2+} ions can be removed by washing with water. Addition of H_2SO_4 is very important step in the preparation of MnO_2. Its importance will be evident from the capacitance measurements. The remaining Mn^{4+} ions present in aqueous solution are dried in two different ways yielding the xerogel and ambigel forms of MnO_2.

Fig. 2 shows the TGA curves of xerogel and ambigel forms of MnO_2 prepared from $NaMnO_4$ as the starting material, in the temperature range of 30–800 °C which depict typical water loss behavior. The xerogel and ambigel showed total weight loss of 28 and 20%, respectively, in the given temperature range. Both forms lose physically adsorbed water in the 30–250 °C temperature range. The xerogel form exhibited a phase transition around 550 °C and another transformation was observed around 800 °C. These findings are in agreement with other research results [17,19]. In contrast to the xerogel form, the ambigel form of MnO_2 did not show any phase transformation. In order to understand this behavior, TGA was done under different temperature increment rates ranging from 20 to 1 °C/min. The ambigel did not show any transformation at any temperature increment rate. This indicates that the phase transitions are not limited by the time scale of experiment.

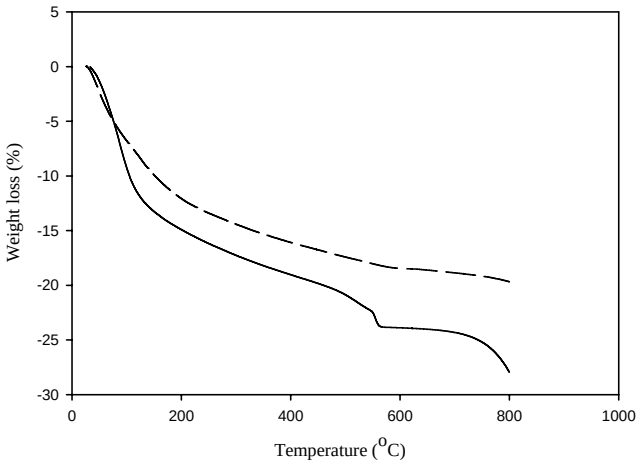

Fig. 2. TGA curves of xerogel (—) and ambigel (– –) form of MnO_2 which is prepared from $NaMnO_4$.

From the combined result of ICP–EC, TGA and chemical titrations, the chemical formula of ambigel form of MnO_2 prepared from $NaMnO_4$ as the starting material was found to be $Na_{0.35}MnO_{2.02}{\cdot}0.75H_2O$. Xerogel and ambigel forms of this material have surface areas of 63 m^2/g and 72 m^2/g, respectively, as determined by BET method. Fig. 3 shows the XRD pattern of the ambigel form of $Na_{0.35}MnO_{2.02}{\cdot}0.75H_2O$, broadening of peaks indicates the amorphous nature of ambigel. Fig. 4 shows the SEM picture of ambigel form of $Na_{0.35}MnO_{2.02}{\cdot}0.75H_2O$. The particles have of different shapes, mostly faceted with an average size of about 5 μm. The chemical formula of the ambigel form of MnO_2 prepared from $KMnO_4$ as the starting material was found to be $K_{0.32}Na_{0.13}MnO_{1.92}{\cdot}0.78H_2O$. The presence of sodium in the material was due to the incorporation of sodium ions from the reducing agent sodium fumarate present during the gelation.

3.1. Electrochemical characterization

3.1.1. $Na_{0.35}MnO_{2.02}{\cdot}0.75H_2O$

Fig. 5a shows the comparison of the cyclic voltammetric curves of the xerogel and ambigel forms of $Na_{0.35}MnO_{2.02}{\cdot}0.75H_2O$ in 2 M NaCl electrolyte. CV curve shows the near ideal rectangular shape without any peaks which indicates that charging and discharging took place at a constant rate over the voltage range of 0.0–1.0 V, which is an indication of capacitative nature [2,20]. Specific capacitance of 130 F/g and 73 F/g were obtained for the ambigel and xerogel forms, respectively. The xerogel form has a lower capacitance compared to the ambigel form. It is interesting to note that there is not much difference in surface area of the xerogel (63 m^2/g) and the ambigel (72 m^2/g). This indicates that the specific capacitance does not depend on the surface area. Pore size distribution may be a deciding parameter in determining the specific capacitance. Generally, these materials have three types of pore distributions, they are micropores, misopores and macropores in the order of increasing of their pore diameter. Ambigel MnO_2 prepared by sol–gel methods has most of the pore volume in the range of misopores with pore diameter ranging from 20 to 100 nm [17], while the xerogel has the most pore volume in the form of micropores with pore diameter <20 nm [17]. The ambigel form might have relatively more accessibility to the electrolyte for surface adsorbtion and intercalation than xerogel.

Fig. 5b shows the effect of the type of electrolyte on the CV curves of the ambigel form of $Na_{0.35}MnO_{2.02}{\cdot}0.75H_2O$. The electrolytes used were 2 M of NaCl, KCl, LiCl and 1 M Na_2SO_4. Table 1 shows the specific capacitance of ambigel from in different electrolytes. As evident from Fig. 5b, ambigel form yielded the highest specific capacitance in

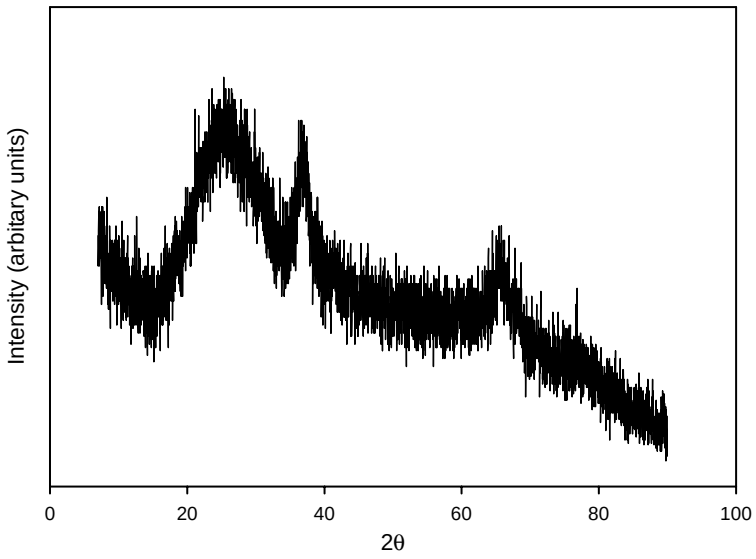

Fig. 3. XRD pattern of ambigel form of $Na_{0.35}MnO_{2.02}{\cdot}0.75H_2O$.

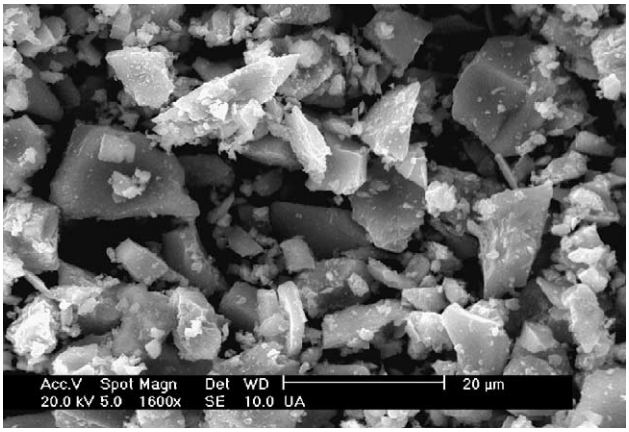

Fig. 4. SEM picture of ambigel form of $Na_{0.35}MnO_{2.02}{\cdot}0.75H_2O$.

2 M NaCl electrolyte. The capacitance arises due to the intercalation of alkali ions into the MnO_2 structure causing redox transitions. Since water is a solvent, alkali ions are surrounded by the water of hydration. Table 2 gives the ionic radius, radius of water of hydration, free energy formation of water of hydration and conductivity of Li, Na, K ions [2,21,22]. The radius of hydration sphere decreases in the order: $Li^+ > Na^+ > K^+$. Li^+ and Na^+ ions have larger hydration spheres when compared to K^+ ion because of the $Li^{\delta+}$–$H_2O^{\delta-}$ and $Na^{\delta+}$–$H_2O^{\delta-}$ strong interactions. But the overall radius of water hydration of all ions is of the same order ranging from 3.3 to 3.8 Å. So, size of the hydration sphere may not be a deciding factor. Potassium ions have distinctly higher conductivity when compared to sodium ions and sodium ion has a higher conductivity than lithium ion.

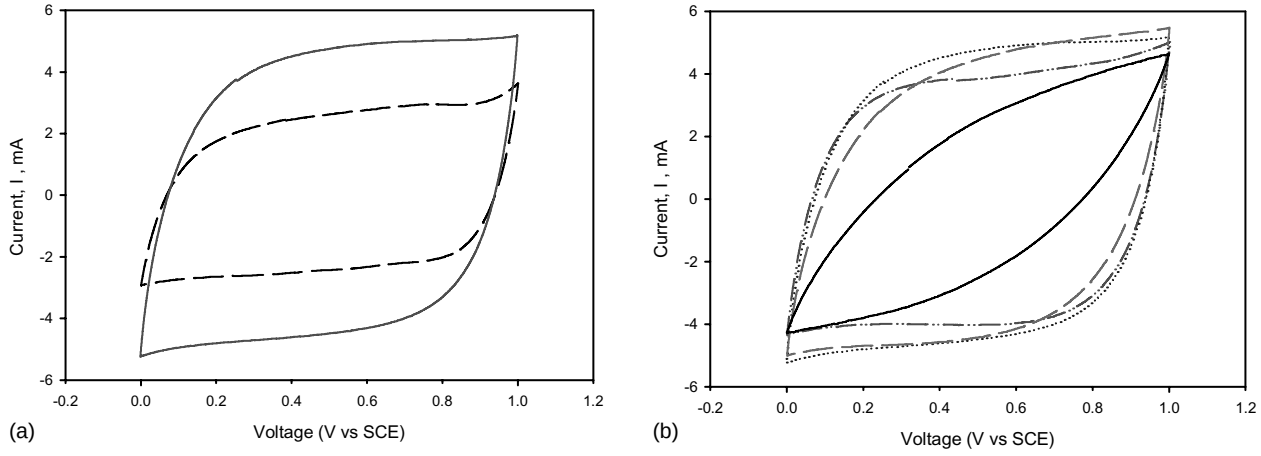

Fig. 5. CV curve of: (a) xerogel (––) and ambigel (—) forms of $Na_{0.35}MnO_{2.02}{\cdot}0.75H_2O$ in 2 M NaCl electrolyte; (b) ambigel form of $Na_{0.35}MnO_{2.02}{\cdot}0.75H_2O$ in 2 M NaCl (···), 1 M Na_2SO_4 (- - -), 2 M KCl (-···) and 2 M LiCl (—) electrolyte.

Table 1
Specific capacitance of ambigel form of $Na_{0.35}MnO_{2.02}\cdot 0.75H_2O$ in different electrolytes

Electrolyte	Specific capacitance (F/g)
LiCl	59
NaCl	130
Na_2SO_4	114
KCl	109

The concentration of Na_2SO_4 is 1 M and rest of the electrolytes concentration is 2 M.

Table 2
Crystal radius, radius of hydration sphere, free energy of hydration, conductivity of alkali ions

Alkali ion	Crystal radius (Å)	Radius of hydration sphere (Å)	Gibbs energy (kcal/mol)	Conductivity (cm^2/Ω mol)
Li^+	0.6	3.82	138.4	38.6
Na^+	0.95	3.58	162.3	50.1
K^+	1.33	3.31	179.9	73.5

Free energy data is relative to H^+ ion hydration; conductivity data corresponds to molar ionic conductivity in water solution at 25 °C.

Conductivity decreases in the order: $K^+ > Na^+ > Li^+$, due to a decrease in the mobility of the ions. Conductivity and mobility of cations may be the determining factor for behavior in different electrolytes. In the case of LiCl, it is clear that the Li^+ ion has a lower conductivity and low mobility leading to non-capacitative behavior. In the case of Na_2SO_4, when compared to NaCl, the sulfate anion is bigger than the chloride anion, which reduces the mobility of Na^+ ion yielding lower capacitance [15]. In case of KCl and NaCl, the Na^+ ion yield higher specific capacitance despite the lower conductivity of the sodium ion. Similar results were obtained by Jeong and Manthiram [15] for MnO_2 which is prepared by reduction of $KMnO_4$ by various reducing agents and they found the highest capacitance in the NaCl electrolyte when compared to the other electrolytes such as KCl, LiCl and Na_2SO_4.

Earlier, Lee at al. reported highest the capacitance in 2 M KCl when compared to 2 M NaCl and 2 M LiCl for amorphous MnO_2 [13]. They attributed this result to the higher mobility of K^+ ion due to its smaller hydration sphere size. Fig. 6a shows the effect of NaCl solution concentration on the ambigel form of $Na_{0.35}MnO_{2.02}\cdot 0.75H_2O$. As can be seen the ambigel form yielded the same capacitance in 2 M and 1 M NaCl solutions, which indicates that the electrolyte might have reached its saturated concentration at 1 M solution. A specific capacitance of 138 F/g was observed in 1 M NaCl electrolyte.

3.2. Capacitance mechanism and role of H_2SO_4 addition in the preparation

In the preparation of manganese oxide, H_2SO_4 is added for conversion of Mn^{3+} ions present in solution to Mn^{4+}. Fig. 6b shows CV curve of MnO_2 without the treatment of H_2SO_4 in 2 M KCl electrolyte at a scan rate of 5 mV/s in the voltage range of −0.2–1.0 V. The material did not show capacitative behavior and yielded a very low specific capacitance of 2 F/g, which indicates capacitance is double layer in nature. The addition of H_2SO_4 led to an almost 55-fold increase in specific capacitance to 109 F/g in the same electrolyte and scan rate for the ambigel form. This indicates that capacitance of the ambigel form of $Na_{0.35}MnO_{2.02}\cdot 0.75H_2O$ is of a pseudo-capacitative nature.

3.3. Ambigel form of $K_{0.32}Na_{0.13}MnO_{1.92}\cdot 0.78H_2O$

Fig. 7 shows CV curves of the ambigel forms of $Na_{0.35}MnO_{2.02}\cdot 0.75H_2O$ and $K_{0.32}Na_{0.13}MnO_{1.92}\cdot 0.78H_2O$. There is no significant difference in the CV curves. This

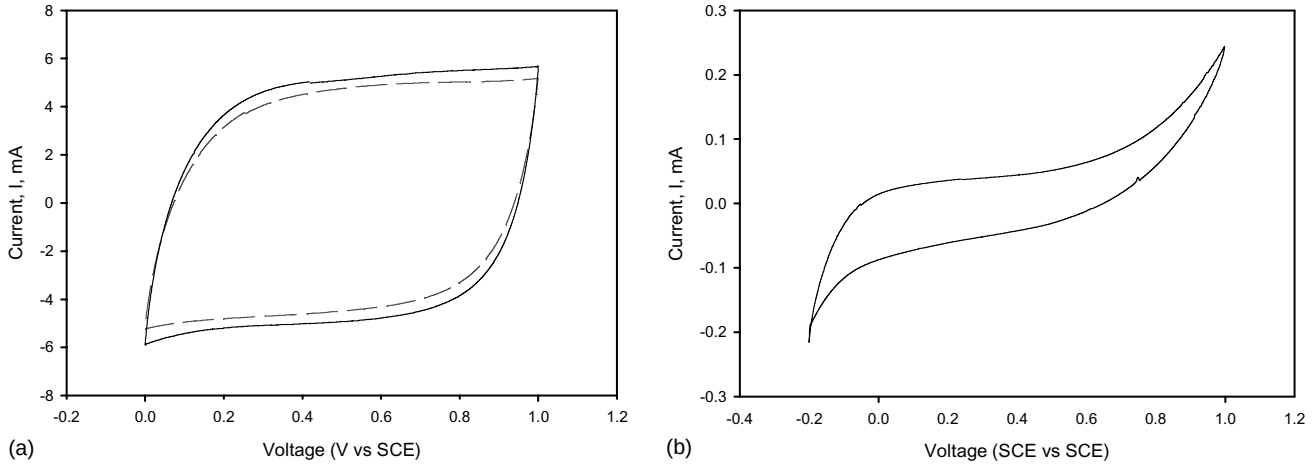

Fig. 6. CV curves of: (a) ambigel form of $Na_{0.35}MnO_{2.02}\cdot 0.75H_2O$ in 2 M NaCl (––) and 1 M NaCl (—) electrolyte; (b) MnO_2 without the treatment of H_2SO_4 in 2 M KCl.

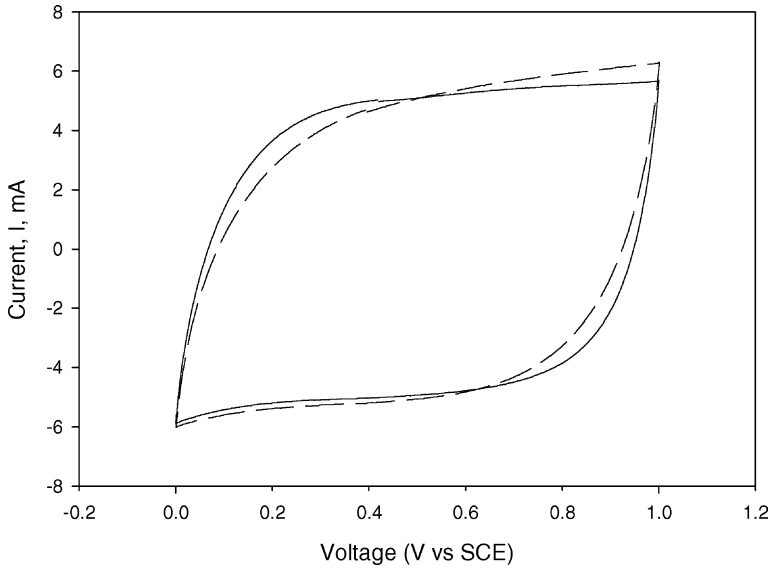

Fig. 7. CV curve of ambigel form of $K_{0.32}Na_{0.13}MnO_{1.92}\cdot 0.78H_2O$ (– –) and $Na_{0.35}MnO_{2.02}\cdot 0.75H_2O$ (—) in 2 M NaCl electrolyte.

indicates that alkali ions present in the MnO_2 lattice act as stabilizing agents for the lattice. Fig. 8a shows the stability of the $K_{0.32}Na_{0.13}MnO_{1.92}\cdot 0.78H_2O$ with cycling. Specific capacitance with cycling is shown in Fig. 8b. The capacitance starts fading after 200 cycles. Capacity fading can be attributed to the slow dissolution of the Mn in the form of Mn^{2+} into the electrolyte due to the disproportionation of the Mn^{3+} in to Mn^{4+} and soluble Mn^{2+} [23,24].

Work is underway to stabilize the MnO_2 structure by the partial substitution of Mn with other transition metals. Comparison of the specific capacitance of MnO_2 in the present study with other researchers was presented in Table 3. Fig. 9 shows the CV curve of carbon black in 2 M NaCl electrolyte at 5 mV/s scan rate. The weight of the carbon black present was 10 mg. The specific capacitance was 3 F/g, which is insignificant. So, we can conclude that the contribution of carbon black is negligible to the total capacitance. Carbon black acts as conductive filler for the active material MnO_2 electrode material.

The following are the reasons for the pseudo-capacitative nature of MnO_2.

(1) Addition of sulfuric acid in the preparation of MnO_2 facilitated the increase of specific capacitance by 55-fold.
(2) Non-capacitative behavior of $Na_{0.35}MnO_{2.02}\cdot 0.75H_2O$ in LiCl, but the capacitative behavior in the NaCl, Na_2SO_4 and KCl electrolytes.

Double layer capacitance will be present in all the materials but its contribution to the total capacitance is minimal.

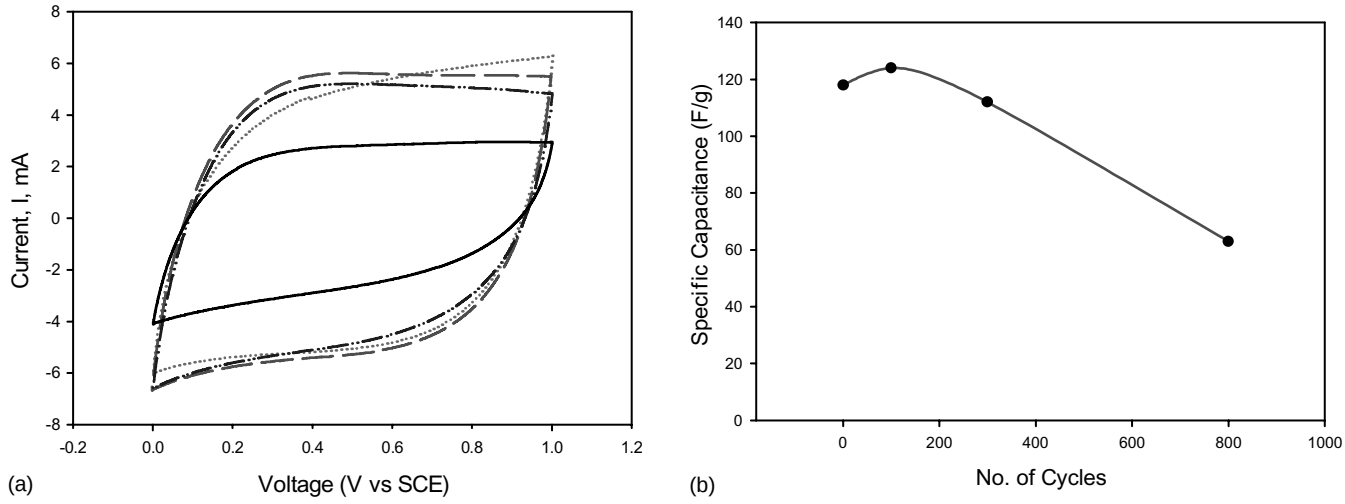

Fig. 8. (a) CV curves of ambigel form of $K_{0.32}Na_{0.13}MnO_{1.92}\cdot 0.78H_2O$ in 1 M NaCl at first cycle (···), 100th cycle (- - -), 200th cycle(- · - ·), 800th cycle (—). (b) Specific capacitance vs. number of cycles.

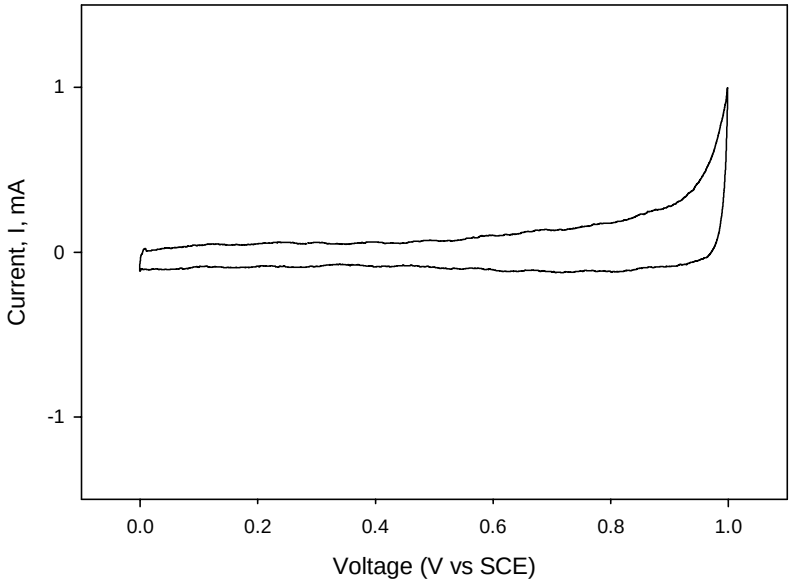

Fig. 9. CV curve of carbon black in 2 M NaCl solution at 5 mV/s scan rate.

Table 3
Comparison of specific capacitance of MnO_2 in the present study with the other researchers

	Specific capacitance (F/g)	Electrolyte	Scan rate (mV/s)
Present study	138	1 M NaCl	5
Jeong and Manthiram [15]	250	2 M NaCl	2
Lee et al. [14]	144	1 M KCl	2
Lee et. al. [13]	240	2 M KCl	5

4. Conclusions

MnO_2 is prepared from a sol–gel method in two different forms as: xerogel and ambigel. The ambigel form of MnO_2 gave higher capacitance when compared to the xerogel from which can be attributed to different pore size distribution present in the two materials. The ambigel form of MnO_2 showed the highest capacitance in 2 M NaCl electrolyte compared to other electrolytes such as KCl, LiCl and Na_2SO_4. Maximum capacitance of 130 F/g was obtained at a scan rate of 5 mV/s for the ambigel form of $Na_{0.35}MnO_{2.02}{\cdot}0.75H_2O$ in a 2 M NaCl solution. This phenomenon can be explained easily in the case of LiCl electrolyte by the conductance and mobility of the lithium ion. Interestingly, Na^+ ion containing electrolytes NaCl and Na_2SO_4 yielded higher capacitance than KCl electrolyte. The ambigel form of $Na_{0.35}MnO_{2.02}{\cdot}0.75H_2O$ yielded almost the same capacitance in 1 M and 2 M NaCl electrolytes, this indicates that the saturated concentration is reached at 1 M NaCl. The ambigel form of $Na_{0.35}MnO_{2.02}{\cdot}0.75H_2O$ yielded maximum specific capacitance of 138 F/g in 1 M NaCl electrolyte. Fading of capacitance in MnO_2 is observed after 200 cycles and it can be attributed to the slow dissolution of Mn in the form of Mn^{2+} ions in to the electrolyte.

Acknowledgements

The authors are thankful for the financial support provided by National Science Foundation Grant no. ECS-0099853. The authors are glad to acknowledge Betsy Graham for ICP–EC and MINT center for XRD. Special thanks to Dr. Divakar Mantha for reviewing this manuscript.

References

[1] R. Kotz, M. Carlen, Electrochem. Acta 45 (2000) 2483.
[2] B.E. Conway, Electrochemical Supercapacitors, Kluwer Academic/Plenum Publishers, New York, 1999.
[3] B.E. Conway, J. Electrochem. Soc. 138 (1991) 1539.
[4] S. Sarangapani, B.V. Tilak, C.P. Chen, J. Electrochem. Soc. 143 (1996) 3791.
[5] R.A. Huggins, Solid State Ion. 134 (2000) 179.
[6] A. Nishino, J. Power Sources 60 (1996) 137.
[7] R.N. Reddy, R.G. Reddy, Electrochemical Capacitor and Hybrid Power Sources, in: R.J. Brodd, D.H. Doughty, K. Naoi, M. Morita, C. Nanjundiah, J.H. Kim (Eds.), Nagasubramanian, PV 2002-7, The Electrochemical Society Proceedings Series, Pennington, NJ, 2002, p. 197.
[8] R.N. Reddy, R.G. Reddy, 2002 EPD Congress and Fundamental of Advanced Materials for Energy Conversion, in: D. Chandra, R.G. Bautista (Eds.), The Minerals, Metals & Materials Society, Philadelphia, 2002, p. 75.
[9] J.P. Zheng, T.R. Jow, J. Electrochem. Soc. 144 (1997) 2417.
[10] J. Suryanarayan, M.S. Thesis, The University of Alabama, Alabama, 2001.
[11] J.P. Zheng, T.R. Jow, J. Electrochem. Soc. 144 (1997) 2026.

[12] J.P. Zheng, T.R. Jow, Electrochem. Solid-State Lett. 2 (1999) 359.
[13] H.Y. Lee, V. Manivannan, J.B. Goodenough, C.R. Acad. Sci., Paris, t. 2, Series IIc, 1999, p. 565.
[14] H.Y. Lee, S.W. Kim, H.Y. Lee, Electrochem. Solid-State Lett. 4 (2001) A19.
[15] Y.U. Jeong, A. Manthiram, J. Electrochem. Soc. 149 (2002) A1419.
[16] S. Bach, M. Hendry, N. Baffier, J. Livage, J. Solid State Chem. 88 (1990) 325.
[17] J.W. Long, R.M. Stroud, D.R. Rolison, J. Non-Crystalline Solids 285 (2001) 288.
[18] S. Franger, S. Bach, J.P. Pereira-Ramos, N. Baffier, Ionics 6 (2000) 470.
[19] S. Franger, S. Bach, J. Farcy, J.P. Pereira-Ramos, N. Baffier, J. Power Sources 109 (2002) 262.
[20] H.Y. Lee, J.B. Goodenough, J. Solid State Chem. 144 (1999) 220.
[21] B.E. Conway, Ionic hydration in chemistry and biophysics, Elsevier, Amsterdam, 1981, p. 73.
[22] P.W. Atkins, Physical Chemistry, third ed., W.H. Freeman and Company, New York, 1986.
[23] R.J. Gummow, A. de Kock, M.M. Thackery, Solid State Ion. 69 (1994) 59.
[24] K. Nishimura, T. Douzono, M. Kasai, H. Andou, Y. Muranaka, Y. Kozono, J. Power Sources 81–82 (1999) 420.